High-rate Manufacturing of 3D Products with Micro and Nanostructured Surfaces

C. Barry and J. Mead
Nanomanufacturing Center, University of Massachusetts, Lowell, MA, USA, carol_barry@uml.edu

Abstract

Injection molding permits the manufacturing of complex three-dimensional products with micro and nanostructured surfaces in less than 30 seconds. Successful high-rate manufacturing of these surfaces depends on understanding the changes required in material selection, tool design and fabrication, and polymer processing parameters. Although temperatures and pressures are greater than with convention injection molded parts, material selection significantly affects the critical processing parameters. Moreover, polymer-tooling interactions, tooling surface roughness, and heat transfer in the tooling used for these surfaces impacts product quality. Finally, material selection and molded-in stress affect interactions with biological species.

Introduction

Micro and nanostructured surfaces impart additional functionality to relatively thick polymer parts. These parts have applications in diagnostics, drug discovery, sensors and actuators, analytical chemistry and biochemistry, superhydrophobic surfaces, micro and nano-mechanics, and micro/nano-optics [1-2]. Elastomeric micro and nano-structured surfaces can provide tuning of friction behavior, flexible patterning, and patterned adhesives [3]. As illustrated in Figure 1, one major approach for high-rate manufacturing of parts with micro and nanostructured surfaces is injection molding. Successful injection molding of these surfaces, however, depends on understanding the changes required in material selection, tool design and fabrication, and polymer processing parameters.

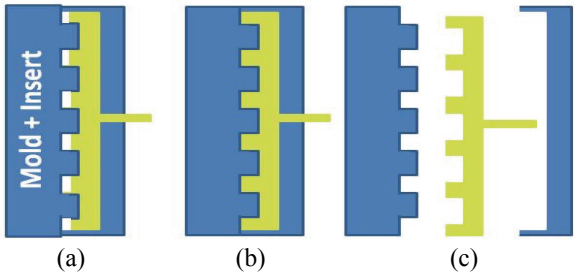

Figure 1. Injection molding of polymer parts with micro and nanostructured surfaces: (a) filling of the mold with polymer melt, (b) "packing" to complete filling of the features, and (c) part ejection after melt solidification. The typical cycle time is less than 30 seconds.

Material Selection

Most injection molding of micro and nanostructured surfaces has been performed using amorphous thermoplastics, such as polymethylmethacrylate polystyrene, polycarbonate, and cyclic olefin polymers (COC, COP). These materials solidify gradually and exhibit similar shrinkage in the microfeatures and the macroscale parts. With amorphous polymers, replication of feature depths or heights depends on melt viscosity, whereas replication of feature details, like the bottoms of microfluidic channels, improves with longer solidification times [4]. Semi-crystalline thermoplastics, however, solidify more rapidly, making micro and nanofeature replication more difficult. The surface features also show shrinkage that is unpredictable and usually much greater than observed in macroscale parts. Replication in both amorphous and semi-crystalline thermoplastics is improved with high melt temperatures, high mold temperatures, high pack pressures, and sometimes, high injection velocities.

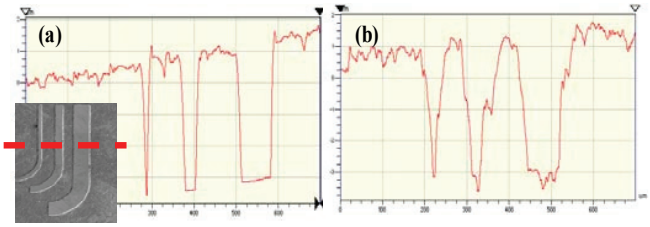

Figure 2. Optical profilometry of injection molded 17 to 84-mm-wide channels, showing the shrinkage of (a) amorphous and (b) semi-crystalline polymers.

With amorphous and semi-crystalline polymers, lower viscosity melts provide better replication. The lower limits for feature dimensions are not clear, but there are indications that they are limited by the size of the polymer molecules. When molding 140-nm features, Srirojpinyo [5] showed that depth ratios decreased with increasing radius of gyration, R_g, of the polymer ; PMMA with an R_g of 3.9 nm provided a depth ratio of 0.91, whereas the depth ratio was 0.60 for polystyrene with a R_g of 14 nm. Polymer melts also should be relatively free of low molecular weight species such as additives and residual monomer. The high stresses during injection molding force low molecular weight materials to the mold surface, causing defects in subsequent parts.

Thermoplastic elastomers behave very differently. Feature replication, especially depth ratio (i.e., the feature depths in the parts relative to feature heights in the tooling) is influenced by hard segment content in the elastomer hardness, and not by viscosity as occurs with conventional thermoplastics [6]. Feature definition (i.e., the shape of the molded feature relative to the feature shape in the tooling) also seems to depend on hard segment content of the elastomers. Softer thermoplastic elastomers - i.e., with lower hard segment content - exhibit better feature definition. Softer elastomers

also required lower melt and mold temperatures for molding [6-7].

Tooling Design

Extensive tooling and tooling fabrication development has been required to meet the sizes and geometries used in parts with micro and nanostructured surfaces. CNC machining of steel is limited to features sizes greater than 100 µm, whereas micromilling and micro-wire electro discharge machining can produce smaller (~25 and 10 µm, respectively) features in steel which typically can withstand more than 1,000,000 molding cycles. Laser machining can create submicrometer-sized features in a variety of substrates, but does not always permit the "closed" tooling features required for injection molding. Lithography and etching techniques, adopted from semiconductor fabrication, provide less robust silicon (Figure 3a), silicone, and resist tooling with features as small as 10 nm. The patterned silicon or photoresist substrate is often electroformed to create metal tooling with an expected life of 40,000-100,000 cycles (Figure 3b). As shown in Figure 3c, larger features can etched directly into steel, but grain size is an issue. Novel tooling has been produced by used the etched silicon to emboss the pattern into a polymer film which is then coated with metal (Figure 3d) [8]. Anti-stiction coatings added all tooling substrates improve filling and part ejection.

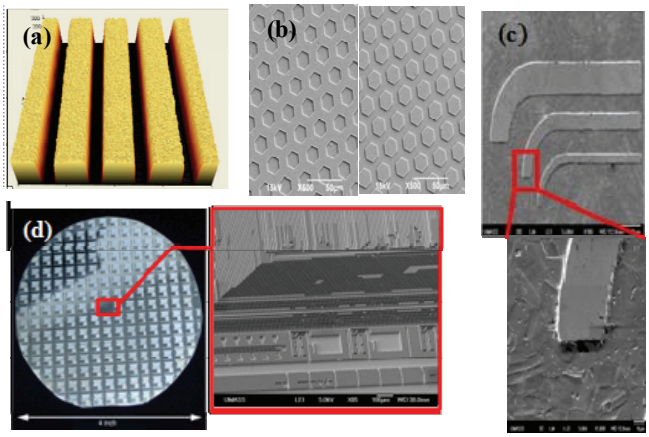

Figure 3. Tooling with micro and/or nanostructured surfaces: (a) silicon, (b) electroformed nickel, (c) etched steel, and (d) novel polymer-metal hybrid tooling.

Tooling design also affects surface replication. First, positive tooling - i.e., tooling with projections in its surface - provides better replication than negative tooling - i.e., tooling with depressions in its surface. For example, a polyurethane exhibited depth ratios of 1.00 and 0.60, respectively, with similar positive and negative tooling [9]. Even with vacuum venting, polymer melt does not easily flow into depressions in the tooling. Second, smaller features are more difficult to replicate. Third, feature spacing affects filling [10]. As shown in Figure 4, complete replication of negative tooling occurred when spacing-to-feature size ratio was 1:1. With a spacing ratio of 2:1, the depth ratio was also 1.00, but top corners of the features were incomplete (conical). When the spacing ratio was 0.5:1, however, the features were had a depth ratio of 0.80. For tightly-spaced feature, these effects were attributed to insufficient filling pressure, whereas non-uniform heat transfer may be the issue with the widely-spaced features.

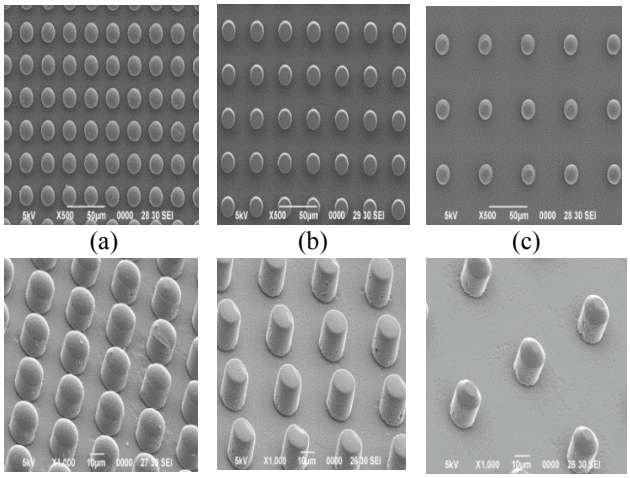

Figure 4. Replication of 20-µm-diameter features with spacing of (a, d) 10 µm, (b, e) 20 µm, and (c, f) 40 µm. The SEM images were obtained at angles of 0° (top) and 45° (bottom).

Tooling with micro and nanostructured surfaces usually is an insert into a steel mold. Flow of the polymer melt in this mold affects replication of the tooling surfaces. When melt can flow directly into the features, filling occurs during the injection stage. In contrast, when melt can flow across the features, the melt hesitates - i.e., stops flowing into the features - until the pressure significantly increases; thus, the features are often filled during the packing stage. For example, direct flow of melt into negative tooling produced clean 1-µm-diameter, 1-µm-high features (Figure 5a),whereas indirect flow of the melt created 0.4-µm-high features with the white caps typical of hesitation (Figure 5b) [11]. Since flow of melt directly into the features leaves a gate vestige amid with features, the hesitation-prone indirect flow is preferred.

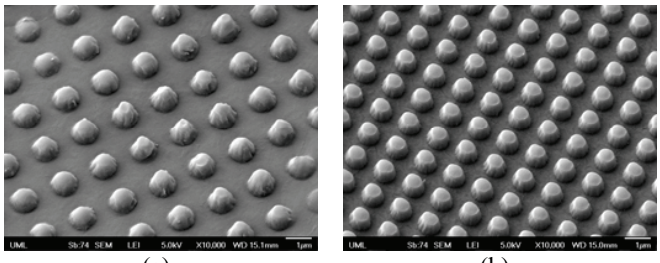

Figure 5. Replication of 1-µm-diameter negative tooling features by (a) direct and (b) indirect flow of the polymer melt. Hesitation occurred with indirect (impingement) flow.

With this indirect flow, positive tooling features also can block flow of the polymer melt [12]. Figure 6a presents the depth ratios for 17, 40, and 84-µm-wide-channels with a 0.15

mm round as a function of channel position. The channels with the highest depth ratios (0.99) were obtained from tooling features which had an angle opened in the direction of flow (T.F.1). In contrast, the channels with the poorest depth replication (T.F.2) had no angle opened to the oncoming flow front; this design prohibited flow into the features. Although the I.F.1 and I.F.2 tooling features groups were oriented in the direction of flow, the channels had intermediate depth ratios (~0.94-0.96). Changing the channel design to a 15° chamfer produced a significant change in replication (Figure 6b). The in-flow channels (I.F.1 and I.F.2) had greater depth ratios than the channels that were transverse to flow (T.F.1 and T.F.2). With the change in channel design, the transverse tooling features blocked the melt flow and the wider "first-contact" feature in T.F.2 provided better blocking of that flow. As expected, the wider channels in all cases showed greater overall depth ratios than did the narrower channels.

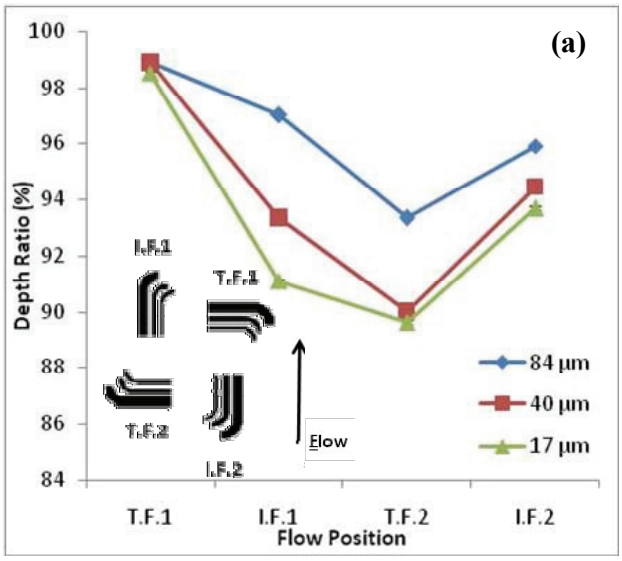

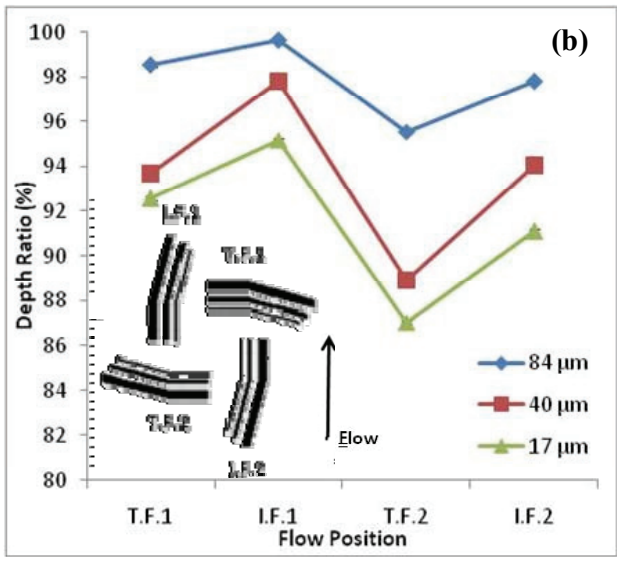

Figure 6. Depth ratios for PMMA microchannels with (a) 0.15 mm round and (b) 15° chamfer as a function of orientation to flow: in-line with flow (I.F.) and transverse to flow (T.F.).

Heat transfer through the tooling impacts feature replication. Rapid cooling of the tooling surface - and solidification of the melt at the surface - prevents complete replication of features. Since stainless steel has a relatively low thermal conductivity (~16 W/m-K), placing an insulator (polymer sheet) behind the stainless steel insert does not affect replication. As shown in Figures 7a and 7b, the depth ratio was about 1.00, but the edge definition of the features was poor. In contrast, nickel has a much greater thermal conductivity (~91 W/m-K). When the nickel tooling is in direct contact with the steel mold, melt cools within 1 second, resulting in a depth ratio of 0.99 and poor edge definition (Figure 7c). Retarding heat transfer by backing the nickel insert with a polymer sheet permitted no real change in depth ratio, but a significant improvement in edge definition (Figure 7d). With smaller and higher aspect ratio features, slowing heat transfer also improves the depth ratio. Insulating between features using the polymer-metal hybrid tooling shown in Figure 3d increases the solidification time from 1 second to about 6 seconds. This change provides better replication than occurs than with polymer-backed nickel tooling.

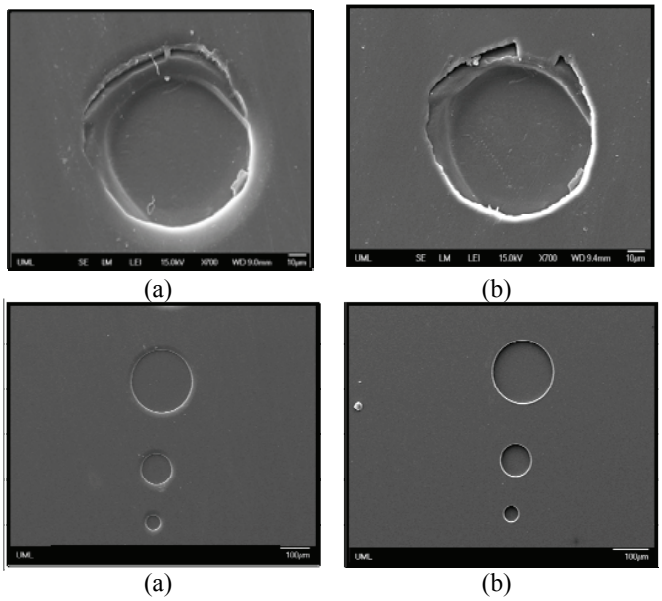

Figure 7. Replication of 200-µm-diameter features molded with (a) uninsulated and (b) insulated stainless steel tooling as well as 150, 200, and 250-µm-diameter features molded with (c) uninsulated and (b) insulated nickel tooling.

The poor replication from the steel tooling in Figures 7a and 7b was due to the differences in roughness and surface tension of the stainless steel compared to the nickel. The nickel tooling was slightly smoother with a surface roughness of 305 nm, whereas the roughness of the stainless steel tooling was 405 nm. Small differences in surface roughness have can affect replication. Melt does not flow well over a too-smooth surface, air is trapped along the surface, and sticking to the surface during part ejection can damage the features. Slightly rough surfaces improve the flow of the polymer melt along the

surface and prevent trapped air. Further increases in roughness, however, hinder replication and part ejection. There is no consensus on the optimum roughness because the effects of roughness are complicated by the surface tension at the tooling surface. This surface tension affects the wetting of the tooling by the polymer melt. For Figure 7, the stainless steel also produced a contact angle of 76° compare to 58° for the nickel tooling; (the fluid used for measurement was water). These measurements suggest that the steel surface was less polar than the nickel surface, and therefore, more compatible with the non-polar polystyrene melt (contact angle: 82°). Poor wetting of the surface by the melt allows the melt to slip along the surface and provide replication of the features. This slip also facilitates part ejection. The stainless steel and nickel tooling used for the parts in Figure 7 had no anti-stiction coating. Anti-stiction coatings further reduce wetting of the tooling by the melt and significantly improve filling and part ejection [10].

Processing Conditions

Replication of micro and nanostructured surfaces is improved by increasing melt temperature which reduces melt viscosity and slows cooling. High mold temperatures produce more defined structures because they delay the solidification time. Mold temperature typically has a greater influence on replication than melt temperature. Filling at high mold temperatures, followed by rapid cooling of the melt using a second, lower mold temperature, has also improved feature replication. Although higher melt and mold temperatures enhance depth ratio, these processing parameters also promote relaxation of oriented polymer molecules and increase shrinkage. The effect is more pronounced with semi-crystalline polymers.

Processing conditions also affect the residual or molded-stress at the part's micro or nanostructured surface. Higher stresses can produce failure of the surface features. Exposure to solvents and higher temperatures will relieve this stress because they allow relaxation of the polymer chains. This relaxation, however, can produce distortion of the features, and possibly, the part. The higher stresses also adversely impacts the adhesion of biological molecules like proteins (Figure 8) [13] and cells to the structured surface.

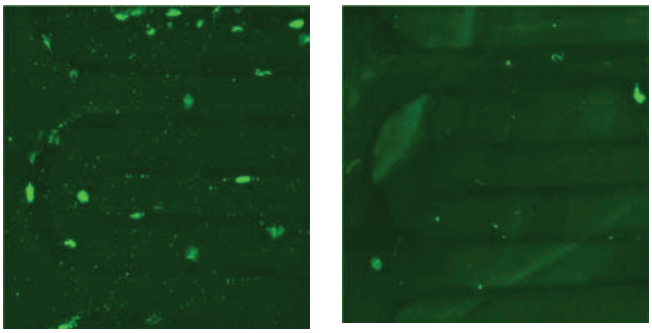

(a) (b)

Figure 8. Confocal micrographs of protein adhesion (light green) to polycarbonate surfaces with (a) low and (b) high residual stress. .

Conclusions

Selection of an amorphous, semi-crystalline, and elastomeric thermoplastic significantly affects the processing conditions needed for good replication of micro and nanostructured surfaces as well as the shrinkage of the features. A wide range of materials and fabrication techniques are used to create tooling for injection molding parts with these structured surfaces. Tooling feature type (positive vs. negative), feature size, and spacing impact replication as does tooling design. Since direct injection into the features provides better replication, but leaves a gate vestige, hesitation-prone indirect (impingement) flow is used to fill the features. Positive features can block this impingement flow. Finally, heat transfer, surface roughness, and wetting of the surface by the melt affect edge definition of micro and nanofeatures.

Acknowledgements

This work was funded by the National Science Foundation (EEC-0832785) and Nypro Inc. The authors also thank Nissei America, Inc.

References

[1] U. Attia, S. Marson, and J. Alcock, Microfluidics and Nanofluidics, 7, 1, 2009.
[2] S. Neethirajan, I. Kobayashi, M. Nakajima, Lab Chip, 11, 1574, 2011.
[3] B. Murarash, Soft Matter, 7, 5553, 2011.
[4] R. Thiruvenkataswamy, S-H. Yoon, J. L. Mead, and C. M. F. Barry, Proc. An. Tech. Conf. Soc. Plast. Eng., 66 2008.
[5] C. Srirojpinyo, D.Eng. Dissertation, University of Massachusetts Lowell, 2005.
[6] Y. Kim, S. Yoon, S-H. Cho, J-G. Park, J. L. Mead, and C. M. F. Barry, Proc. Ann. Tech. Conf. Soc. Plast. Eng., 69, 2011.
[7] M. W. Alabran, D. J. Carter, A. A. Busnaina, J. L Mead, and C. M. F. Barry, Proc. Ann. Tech. Conf. Soc. Plast. Eng., 65, 2007.
[8] S-H. Yoon, P. Padmanabha, J. S. Lee, N. Cha, A. A. Busnaina, J. L. Mead, and C. M. F. Barry, Proc. Ann. Tech. Conf. Soc. Plast. Eng., 66, 2008.
[9] S-H. Yoon, J. Mead, and C. Barry, 176th Technical Meeting, ACS Rubber Division, October 13-15, 2009.
[10] S. Birkar, J-G. Park, J. Mead, and C. Barry, Proc. Ann. Tech. Conf. Soc. Plast. Eng., 72, 2014.
[11] S-H. Yoon, N-G. Cha, J. Lee, J-G. Park, D. Carter, J. Mead, and C. Barry, Polymer Engineering and Science, 50, 411, 2010.
[12] D. Dempsey, N. George, S-H. Yoon, E. Paszkowski, M. McGee, J. L Mead and C. M. Barry, Proc. Ann. Tech. Conf. Soc. Plast. Eng., 69, 2011.
[13] N. George, D. Dempsey, S-H. Yoon, E. Paszkowski, M. McGee, J. L Mead and C. M. Barry, Proc. Ann. Tech. Conf. Soc. Plast. Eng., 69, 2011.